SAND2014-19943D

Materials Characterization and Performance (01819)

Surface Analysis Laboratory – Synchrotron Techniques

Michael T. Brumbach, B.A., M.S., Ph.D.
Sr. Member of Technical Staff
mtbrumb@sandia.gov
(505) 284-2605

James (Tony) A. Ohlhausen, B.S., M.S.
Sr. Member of Technical Staff
jaohlha@sandia.gov
(505) 845-9510

Ana B. Trujillo, B.S.
Technologist
abtruji@sandia.gov
(505) 284-2670

Elizabeth (Liz) M. Huffman, B.S.
Technologist
emhuffm@sandia.gov
(505) 845-8778

James Aubert, Ph.D.
Manager
jhaubert@sandia.gov
(505) 844-4481

Alex J. Mirabal
Student Intern (University of New Mexico)
ajmirab@sandia.gov
(505) 844-2804

Michael A. Kalan
Summer Student Intern (University of Dallas)

NSLS

First operated in 1982, the National Synchrotron Light Source has accommodated more than 18,400 unique users in its lifetime as a Department of Energy user facility. After 32 years of distinguished operations, NSLS was shut down on September 30, 2014. Replacing it is NSLS-II, which, when fully built out, will accommodate 60-70 beamlines and host over 4,000 users every year. On September 30 NSLS had its "Last Light," when the facility was shut down for the last time.

NSLS II

To provide extremely bright x-rays for basic and applied research in biology and medicine, materials and chemical sciences, geosciences and environmental sciences, and nanoscience

Sponsor

U.S. Department of Energy (DOE), Office of Science, Office of Basic Energy Sciences

Costs

$912 million to design and build

Features

State-of-the-art, medium-energy (3-billion-electron-volt, or GeV) electron storage ring that produces x-rays up to 10,000 times brighter than the NSLS

SYNCHROTRON-BASED SURFACE SCIENCE

• UV and X-ray light produced at synchrotrons enables unique opportunities for variable energy and polarized sources

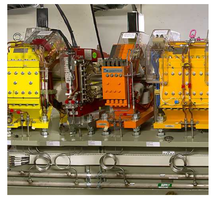

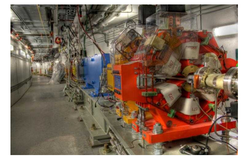

Advanced Synchrotron Measurement Method Development

NIST NSLS-II Spectroscopy Beamline Suite: Soft and Tender and Microscopy

***Soft** and **Tender** Beams Together – 100 eV to 7.5 keV*

NIST Material Measurement Laboratory

"NIST NSLS-II Spectroscopy Beamline Optical Plan for Soft and Tender X-ray Spectroscopy and Microscopy (100 eV to 7.5 keV)" R. Reininger, J.C. Woicik, S.L. Hulbert, D.A. Fischer, Nucl. Instr. and Meth. A, doi:10.1016/j.nima.2010.11.172, (2010).

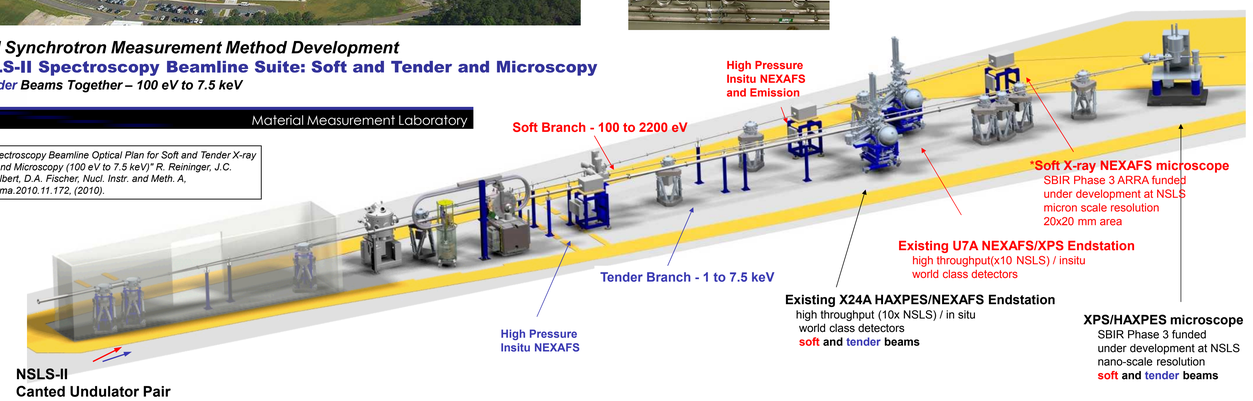

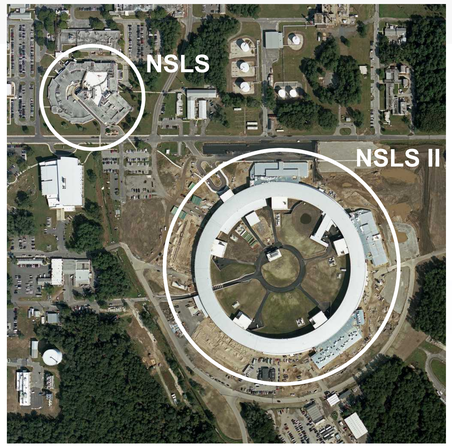

NSLS II - Next generation synchrotron light **(2015)**
10,000 times brighter than NSLS I
High-current electron beam, sub-nm-rad horizontal emittance (0.5 nm-rad) and diffraction-limited vertical emittance (8 pm-rad)
Stable beam position, angle, dimension, intensity
Wide spectral range (0.1 meV ($1cm^{-1}$, far IR) to 300 keV (hard X-ray))

HAXPES

Hard X-ray Photoelectron spectroscopy - core level electrons using a variable energy source

- Non-destructive depth profiling – Buried interfaces – Subtract out contamination layer – Optimize cross section -

VKE-XPS

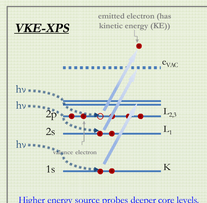

Higher energy source probes deeper core levels.

$$BE = hv - KE - \Phi_{spectrometer}$$

$hv_{UPS} = 21.2$ eV
$hv_{XPS} = 1486.6$ eV
vs.
$hv_{X24A/U7A} = 200$ to 5000 eV

Variable Excitation Energy
(Non-destructive variable depth resolution)

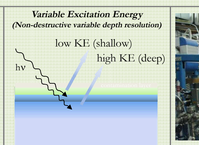

Greater intensity and lower energy dispersion of the source enable high resolution and good S/N.

VKE-XPS of Buried Interfaces

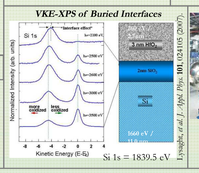

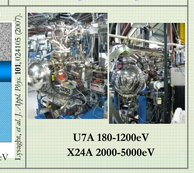

Lysaght, *et al. J. Appl. Phys.* **101**, 024316 (2007).

U7A 180-1200eV
X24A 2000-5000eV

Near Edge X-ray Absorption Fine Structure

NEXAFS measures resonance photoemission

- Ideal for organics C, N, O, F – Chemical state identification – Molecular orientation – Monolayers – Film segregation -

NEXAFS

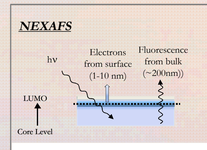

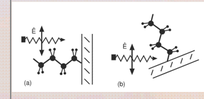

The maximum intensity of transition is achieved when the electric field vector is parallel to the respective bonding orbital; thus, when the beam is normal (a) the dominant transition will be the C-H* and at glancing angle geometry (b) the major transition will be the C-C*.

(*J. Mat. Sci. Let.*, **17** (1998) 1223-1225.)

Molecular Orbital Orientation
Resonance with incoming X-ray

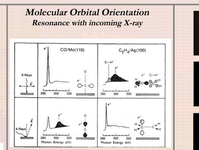

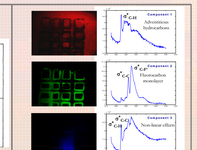

NEXAFS Spectroscopy, Joachim Stöhr, Springer, 2003

NEXAFS

- A synchrotron-generated variable energy X-ray beam (180-1200 eV) irradiates the sample surface.
- A monochromator selects energy and directs the beam to the sample.
- The X-rays at a given energy are absorbed when they match electron energies (resonance).
- The intensity of ejected electrons (or photons) are plotted versus X-ray energy.
- Polarized light from the synchrotron allows for probing of molecular orientation.

U7A
180-1200eV

Imaging Near Edge X-ray Absorption Fine Structure

Imaging NEXAFS scans large areas for analysis of arrays

- Micro-array imaging – Molecular orientation mapping across large area –

Imaging NEXAFS

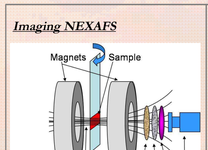

Molecular Orbital Orientation
Resonance with incoming X-ray

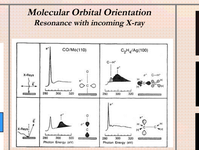

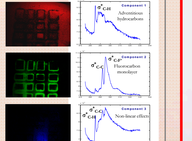

NEXAFS Spectroscopy, Joachim Stöhr, Springer, 2003

NEXAFS

- A synchrotron-generated variable energy X-ray beam (180-1200 eV) irradiates the sample surface.
- A monochromator selects energy and directs the beam to the sample.
- The X-rays at a given energy are absorbed when they match electron energies (resonance).
- Secondary electrons travel along magnetic field lines to a channel plate amplifier then phosphor screen.
- A CCD directly images the phosphor, recording the spatially resolved intensity of ejected electrons.

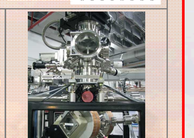

U7A
180-1200eV

Advantages of HAXPES

Study samples from air; i.e., real samples!
Tune λ for experimental system
Variable kinetic energy XPS (VKE-XPS) for depth profiling and chemical speciation
Bulk and surface sensitive core lines accessible for same element
Eliminate Auger interference
Photoemission and other techniques (SSXPS)

JOURNAL OF APPLIED PHYSICS **109**, 114911 (2011)

Activation of erbium films for hydrogen storage

Michael T. Brumbach,[1,a] James A. Ohlhausen,[1] Kevin R. Zavadil,[2] Clark S. Snow,[3] and Joseph C. Woicik[4]
[1]*Materials Characterization Department, Sandia National Laboratories, Albuquerque, New Mexico 87185, USA*
[2]*Applied Science and Technology Department, Sandia National Laboratories, Albuquerque, New Mexico 87185, USA*
[3]*Applied Science and Technology Management Department, Sandia National Laboratories, Albuquerque, New Mexico 87185, USA*
[4]*National Institute of Standards and Technology, Gaithersburg, Maryland 20899, USA*

(Received 17 February 2011; accepted 9 April 2011; published online 15 June 2011)

Hydriding of metals can be routinely performed at high temperature in a rich hydrogen atmosphere. Due to the hydrogen loading process, hydriding at room temperature is not practical. Hydriding gets initiated on a few isolated spots and then spreads to the rest of the activation process. Little is known about the chemical and electronic changes that occur during activation and how they control eventual kinetic rates of hydrogen uptake. This study utilized variable kinetic energy X-ray photoelectron spectroscopy to interrogate the changes during in situ thermal annealing of erbium films with results confirmed by time-of-flight secondary ion mass spectrometry and low energy ion scattering. Activation can be identified by a large drop in surface contamination between the valence band maximum and the Fermi level and appears to occur over a two stage process. The first stage involves desorption of contaminants and recrystallization of the oxide, initially impeding hydrogen loading. Further heating overcomes the first stage and leads to degradation of the passive surface oxide leading to a bulk film more accessible for hydrogen loading. © *2011 American Institute of Physics*. [doi:10.1063/1.3590355]

[a]Author to whom correspondence should be addressed. Electronic mail: mtbrumb@sandia.gov.

0021-8979/11/109(11)/114911/5/$30.00 **109**, 114911-1 © 2011 American Institute of Physics

I. INTRODUCTION

Many transition and rare earth metals are known to be effective at the long-term storage of hydrogen including Er, Zr, Ti, Sc, Ta, V, and W.[1–3] These metals can be hydrided by thermal treatment in a rich hydrogen atmosphere. Metal hydrides are attractive for hydrogen storage because they are many stable and metastable phases have been identified.[4–6] It is well known that prior to the hydrogen loading process an activation procedure is required.[7,8] The activation procedure is a temperature ramp and hold at a high temperature for a short period of time prior to reducing the temperature for H-loading for a longer period of time. If activation is not performed, hydride formation at the bulk film is prohibitively slow.[7] Despite the routine use of the thermal activation process, little is known about the chemical, physical, and/or electronic changes that occur during activation. Results for hydrogen uptake in erbium films are similar to those observed across other rare earth and transition metal systems used for hydrogen storage. Additionally, this work has intentionally evaluated the activation process under similar vacuum conditions as those likely to be encountered in a hydriding system, thereby giving a more accurate description of the activation process as it relates to real applications.

Müller *et al.* have demonstrated the fast rate and large capacity of H_2 gettering for erbium films.[9] Additionally, they found that an erbium film exposed to oxygen would not getter hydrogen, while an erbium film exposed to hydrogen would getter oxygen.[9] Sowell and King performed an investigation on the stability of erbium trihydride with some insights on the activation of erbium.[7] The passive surface oxide ubiquitously observed for erbium was proposed to act as a capping barrier over a hydrided erbium film, thereby reducing the loss of hydrogen from the film. Therefore, under ambient conditions, they were able to observe the metastable trihydride phase which did not decompose to the stable dihydride as would be expected at room temperature.[7] Auger depth profiles showed oxygen content throughout the bulk of the hydrided erbium film and a reduction in the oxygen level to a substantial degree at the surface. However, the surface had led to a greater concentration of oxygen through the bulk. Hydrogen loading led to a significant increase in total oxygen, at the surface and throughout the bulk, however there was no clear source for oxygen. Parish *et al.* have also observed a thick oxide layer (30–130 nm thick) in their hydrided erbium films. These investigations have demonstrated the importance of the passive surface oxide but do not give clear explanations for the role it plays on the mechanisms of adsorption, dissociation, absorption, and/or desorption of hydrogen.

This work presents a thorough characterization of the activation process. It has determined the mechanisms for defect generation and mediated transport accelerated by the thermal activation step. Variable kinetic energy X-ray photoelectron spectroscopy (VKE-XPS) provides the ability to perform nondestructive depth profiling with high energy resolution to evaluate chemical changes in the near surface region. Valence band (VB) spectra were used to observe electronic changes upon activation. Composition was performed in situ deposition of polymers via electrospray deposition to evaluate the interfacial energy alignment.[10] Hard energy X-ray photoelectron spectroscopy (HAXPES) is well suited to the study of a polymer/substrate interface since a single sample can be used for the entire analysis.

In most circumstances where XPS has been used to characterize indium tin oxide (ITO), the surface has been exposed to atmosphere, and an X-ray source of 1486.6 eV has been used. Although lower excitation energies and angle resolved measurements can be employed to enhance surface sensitivity, surface roughness, adsorption of adventitious species, and/or measurements which are still too bulk sensitive can confound these attempts to evaluate the ITO surface. Additionally, these studies have evaluated the bare ITO surface and the ITO surface with a buried interface. Therefore, the presence of the organic film allowed for the tuning of the high-energy X-rays to act as both a surface-sensitive probe at the ITO surface, as well as a deeper probe into the interface, while in the presence of the organic semiconductor.[11,12] Three cases were examined for the ITO surface were presented to give varying surface chemistries. ITO surface chemistry is known to be highly variable and dependent on how the surface preparation impacts on device performance.[13,14] The depth discrimination accessed by HAXPES allowed for the observation of a very thin,

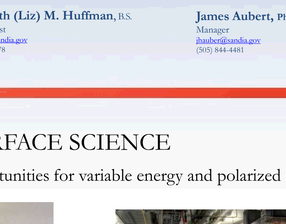

FIG. 1. (Color) The activation of erbium films requires a temperature ramp and hold at an elevated temperature for a short period of time. The temperature is schematically represented by the red line. Initially, the erbium film is covered by a passivating surface oxide. Activation is proposed to occur over a two stage process. The first stage involves desorption of contaminants and recrystallization of the surface oxide, initially impeding hydrogen loading. Further heating overcomes the first stage and leads to degradation of the passive surface oxide leading to a bulk film more accessible for hydrogen loading. The dashed boundary is at or near the surface the film is activated, i.e., the passive oxide is degraded, allowing for hydrogen transport to the surface for H_2 dissociation, as well as for bulk H transport into the bulk.

Research article
Received: 15 February 2012 Revised: 21 May 2012 Accepted: 22 May 2012 Published online in Wiley Online Library: 15 June 2012
(wileyonlinelibrary.com) DOI: 10.1002/sia.3972

HAXPES of protected ITO surfaces at the buried P3HT/ITO interface

Michael T. Brumbach[a]* and Joseph C. Woicik[b]

The characterization of buried interfaces is difficult and often has to be performed by a post-processing method where the interface is exposed. Hard energy X-ray photoelectron spectroscopy offers the ability to tune the X-ray energy and thereby change the information depth. In this work, an inorganic/organic interface was evaluated, namely the poly(3-hexylthiophene) (P3HT)/indium tin oxide (ITO) interface. The P3HT film protected the ITO surface from adventitious adsorbates and allowed for sensitivity to the buried ITO surface. Three cases were examined using three X-ray energies where the ITO surface was prepared under different processing conditions. The P3HT film protected the ITO surface from adventitious adsorbates and allowed for sensitivity to the buried ITO surface. Robust peak fitting routines were developed for the In 3d, O 1s, and C 1s spectra. The ITO surface was found to be highly variable and dependent on the clean identification of a surface layer on the ITO which is oxidized to a greater extent than the underlying bulk ITO. The surface oxide layer, composed of indium oxide and indium hydroxide, is deficient of oxygen vacancies and would therefore be expected to act as an insulating barrier on the ITO surface. Peak fitting conditions allowed for an estimation of the relative thicknesses of this insulating layer. Copyright © 2012 John Wiley & Sons, Ltd.

Keywords: buried interface; P3HT; ITO; XPS; HAXPES; peak fitting

Introduction

The characterization of buried interfaces is of significant interest to the study of organic electronics yielding insights on the interfacial energetics, chemistry, and structure. Common methods for investigation of species at interfaces, and identification of interfacial contaminants,[1,2] is inorganic photovoltaics (OPVs) and organic light emitting diodes, charge injection barriers can be present due to energy level offsets, and also due to the presence of unbeatable species.[3–5] Interfacial chemistry can be substantially altered by the presence of adventitious species have been shown to dramatically affect the performance of organic electronic devices.[6–10] Similarly, work on interfacial oxides has led to increased efficiencies in OPVs.[11,12] Understanding and identifying surface contributions to the bulk properties is therefore important to improve the efficiency of organic electronic devices.

The nature of the interface in real devices is often unknown, since the interface is buried and cannot be directly characterized. For many studies, characterization relies on separate analyses of the two surfaces that will eventually form the interface. The results from the two components are then combined to give a description of the interface and are assumed to remain unchanged when the materials are contacted. More rigorous strategies for evaluating interfaces are to do sequential analyses of the resulting thickness films under highly controlled conditions.[13–15] For the case of contacting polymeric or inorganic surfaces, the interface is often buried under the polymer. Some techniques layers in the absence of adventitious contaminants. Additionally, polymer deposition introduces solvent interactions with the substrate. Recently, a polymer/oxide interface was thoroughly examined by use of multiple samples with varying thickness films.[16] Ideally, a technique that can probe the buried interface would were the same for all samples.[17] *Schlaf and coworkers have also*

* Correspondence to: Michael T. Brumbach, Materials Characterization Department, Sandia National Laboratories, Albuquerque, NM 87185, USA. E-mail: mtbrumb@sandia.gov

a Materials Characterization Department, Sandia National Laboratories, Albuquerque, NM 87185, USA

b National Institute of Standards and Technology, Gaithersburg, MD 20899, USA

Copyright © 2012 John Wiley & Sons, Ltd.

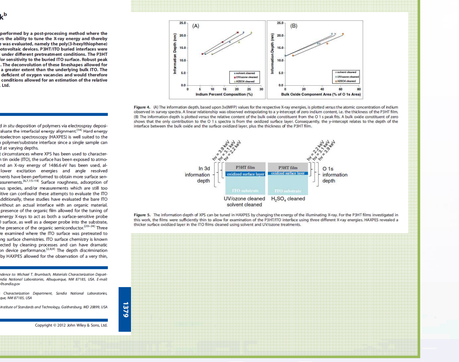

Figure 4. (A) The information depth based upon 3s/BKFP values for the respective X-ray energies, is plotted versus the atomic concentration of indium observed in survey spectra. A linear relationship was observed extrapolating to a x-intercept of zero indium content, as the thickness of the P3HT film. (B) The information depth is plotted versus the relative content of the bulk oxide constituent from the O 1s peak fits. A bulk oxide constituent of zero means that the only contribution to the O 1s spectra is from the oxidized surface layer. Consequently, the y-intercept relates to the depth of the interface between the bulk oxide and the surface oxidized layer, plus the thickness of the P3HT film.

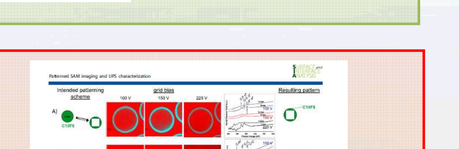

Figure 5. The information depth of XPS can be tuned in HAXPES by changing the energy of the illuminating X-ray. For the P3HT films investigated in this work, the films were sufficiently thin to allow for examination of the P3HT/ITO interface using three different X-ray energies. HAXPES revealed a thicker surface oxidized layer in the ITO films cleaned using solvent and UV/ozone treatments.

Special issue article
Received: 17 August 2012 Revised: 31 January 2013 Accepted: 15 February 2013 Published online in Wiley Online Library: 20 March 2013
(wileyonlinelibrary.com) DOI: 10.1002/sia.5264

Imaging, work function, and compositional changes of thiols on gold via shadow mask ozonolysis

Michael T. Brumbach,[a]* Cherno Jaye,[b] James T. Ohlhausen[a] and Daniel Fischer[b]

Self-assembled monolayers (SAMs) of alkyl and fluorinated thiols were investigated after ozonolysis shadow mask treatments with varying areal densities and after exposure to displacing thiols. Imaging near edge X-ray absorption fine structure (NEXAFS) spectroscopy was used as a novel method for investigating the resulting heterogeneous SAM films. Composition and work function changes were investigated with X-ray photoelectron spectroscopy and ultraviolet photoelectron spectroscopy. The characterization of these heterogeneous films clearly shows the displacement of oxidized thiols after ozonolysis patterning. Changes in the SAM after patterning, and after displacement from back-filling thiols, can be inferred from changes in the carbon 1s spectra. Work function changes were also investigated and are consistent with the trends observed for cases where thiols were displaced after ozonolysis suggesting that the displacing SAM was dense and/or more ordered than as-deposited films. These results highlight one of the first demonstrations of imaging NEXAFS and present new avenues of effective work function on intentionally heterogeneous SAM films. Copyright © 2013 John Wiley & Sons, Ltd.

Supporting information may be found in the online version of this article.

Keywords: NEXAFS; XPS; UPS; imaging; thiol; SAM; pattern; work function

Introduction

The use of self-assembled monolayers (SAMs) to alter the chemistry and work function of surfaces has been well-established.[1–10] Thiols have been extensively studied and are known to form close packed monolayers on gold.[11–14] Numerous studies have been performed to investigate the work function changes of thiols on gold.[15–18] A much smaller set of studies have investigated the changes in the effective work function of the gold substrate by the modifying thiol SAM. Allowing *et al.* have shown that the effective work function of gold can be tuned across a broad energy range (>1 eV) by varying the fluorination of the thiol used for SAM modification.[19] The dipole moment of thiol molecules was also found to correlate with the observed work function changes.[20] In turn, leading to an increase in effective work function in fluorinated thiol SAMs on gold.[19] Alkyl thiols, with dipole moments around +1.5 D, gave a negative shift in the vacuum level, or a decrease in effective work function.[21] These changes in the work function of gold upon thiol SAM formation were also observed by numerous authors and are consistent with the trends observed in this work.[15,16,22] More recently, a number of reports have evaluated the role of mixed thiol SAMs on the effective work function of gold.[23,24] Alloway *et al.* determined a linear correlation between the vacuum level and the relative concentration of a fluorinated thiol in hexadecanethiol SAM films.[24] Additionally, Ishida *et al.* have used mixed SAMs of fluorinated dipole strip to surface potential versus relative concentration of 1H,1H,2H-perfluorodecanethiol in decanethiol SAMs.[23]

These studies have only evaluated the work function of contributions of thiol species in the mixed SAMs and have not intentionally examined any role of spatial organization within the mixed film. In the reports mentioned above, the bimolecular film consisted of randomly mixed, but well-packed thiols using SAMs and XPS.[19,20,23,24] Imaging NEXAFS and UPS have not been previously applied to heterogeneous SAMs on the role of intermolecular or SAM dipole/dipole interactions.

Intentional patterning of SAMs allows for control of the domain sizes while easing the ability to characterize the resulting

* Correspondence to: Michael Brumbach, Materials Characterization, Sandia National Laboratories, New Mexico, 1100, P.O. Box 5800 mtbrumb@sandia.gov

a Sandia National Laboratories, Albuquerque, New Mexico, 87185, USA

b National Institute for Standards and Technology, Gaithersburg, MD, 20899, USA

Copyright © 2013 John Wiley & Sons, Ltd.

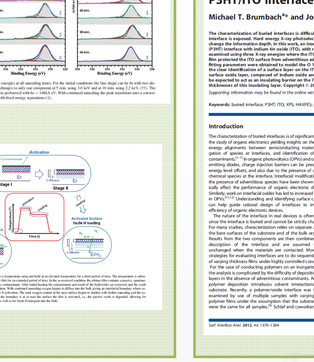

Figure 1. Thiol modification of gold was accomplished by first treating the sample with either decanethiol (C10) or perfluorodecanethiol (C10F). The sample was then exposed to UV/ozone removing each unit without shadow masks to remove all thiol from unmasked regions. One set of thiol-modified surfaces were retained for analysis, while the second set was placed in the alternate thiol solution to backfill the UV/ozone-cleaned regions.

work function was obtained for the *C10F/gold/*C10 films relative to the as-deposited C10/Au film. The C 1s peak for the *C10F/gold/C10 SAM also showed a change C-F component than the as-deposited C10/Au film.

Shadow mask ozonolysis of SAMs

SAMs were patterned using Mrico TEM grids, as previously mentioned, leaving areas of 30%, 46%, 29%, and 23% where as-deposited SAMs were directly exposed to UV/ozone irradiation. Unexposed SAM films were retained for analysis while others were subjected to UV/ozone without a shadow mask to completely remove the SAM and create a uniform hydrophilic surface. This was by far patterned, C10 and C10F/Au SAMs with varying areas of exposure. There was little variation in the UPS spectra in the relative areas for patterning were varied. Additionally, there were only subtle differences between the UPS spectra from patterned C10 and patterned C10F/Au films. The C 1s peak from the patterned C10/Au, Fig. 3D, showed a reduction in the C 1 s peak intensity, relative to the 100% modified surface, and the peak shape varied little over the range of patterned areas. A C-F component was observed in the C 1 s peak for the 100% modified C10F/Au sample, Fig. 3D. However, this component was not observed for the patterned SAM films.

Figure 4A summarizes the changes in work function for the various patterned SAMs and the backfilled samples (see also Figure S1 in the supplemental information). The effective work function was generally lower for the C10-modified gold relative to C10F/Au modified gold across all areas of exposed modification, with the largest differences observed at higher areas of modification. The observed SAM films were retained for analysis while others were subjected to UV/ozone without a shadow mask to completely remove the SAM and create a uniform hydrophilic surface. This was by far the largest change in work function observed in this study. There was still fluorine observed at the surface; however, the conversion of fluorine did not change as the area of SAM modification was varied for all samples exposed to UV/ozone (data not summarized). The Au 4f peak was attenuated in a systematic progression as the area of coverage was varied (supplemental information). It is worth noting that sulfur was observed for all samples; however, given

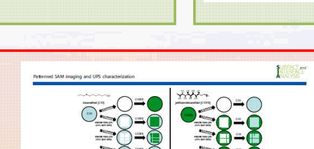

Figure 2. 3D UPS spectra are shown for gold samples which have been: UV/ozone cleaned, sputter cleaned, and for samples modified with either C10 or C10F SAMs (A). The work function changes relative to the UV/ozone cleaned gold are shown in (B). The work function of the C10F/Au film shifts after a C10/Au SAM was removed via UV/ozone cleaning (*C10/gold/C10F/Au). Both were similar. Additionally, UPS spectra were similar for C10/Au modified gold (C10/Au) relative to a C10/Au SAM deposited after a C10 SAM was removed (*C10/gold/C10/gold). (C) C 1s spectra for C10 and for *C10/gold/C10/gold show that the C10/Au hydrocarbon was efficiently removed by ozone exposure steps. C-F components were measured. The C 1 s peak was also measured for *C10/gold/C10/Au films similar to the as-deposited C10/Au. In addition, a C-F component was observed for the *C10/gold/post-C10/Au. The components of high-KE corresponding to C-F core-features, are more pronounced for the *C10/gold/post-C10/Au.

Figure 6. NEXAFS images and the corresponding spectra are shown for three patterning schemes where spectra were recorded using three different beam spotsize to the grid at the entrance to the partial electron yield detector. Regions in bright yellow indicate more surface sensitive images. NEXAFS images and the corresponding spectra for C10/Au films that C10F/Au were retained in the lines of the pattern as expected. For Scheme B, where C10 was used as the backfilling thiol, the C10/Au regions appeared dark relative to the C10F/Au regions. This was consistent with the C10/Au regions displaced by the ex-situ backfilling method C10. This was correspondingly observed for the case where patterned C10 was backfilled with C10F/Au (Scheme C). However, the C10F/Au retained a patterned contrast as assisted with spectral intensity variations of C10F/Au.

Conclusions

UV/ozone shadow mask patterning resulted in the photooxidization of C10 and C10F/ SAMs. C10 SAMs were removed by UV/ozone cleaning in ethanol, while patterned C10F/Au SAMs remained adsorbed to the surface in solvents. Photooxidized SAMs were easily displaced by a secondarily deposited SAM. The secondarily deposited SAMs were found to be more ordered than the as-deposited SAMs. Patterned SAM films deposited initially onto clean gold surfaces, imaging NEXAFS was successfully demonstrated as patterned thiol monolayers. This technique was challenging when examining the patterning process, helping rationalize the observed changes in effective work function. The most significant changes in work function were observed for patterned *C10F/C10/Au SAMs. *C10F/post-C10 where a linear increase in work function was observed with increasing areas of exposed C10/Au. However, this work particularly interesting since the patterned samples showed a higher work function than uniform 100% modified *C10F/post-C10 samples. Additional angle-resolved NEXAFS experiments would help determine if the secondarily deposited SAMs are indeed more uniformly aligned.

Acknowledgements

The authors are grateful for support from Sandia National Laboratories Laboratory Directed Research and Development Program. The inclusion of companey names is for completeness and does not imply endorsement by Sandia National Laboratories or the National Institute of Technology or Sandia National Laboratories. The authors are grateful for support from Sandia National Laboratories.

References

[1] N. K. Venkatramanan, S. Zuerbes, A. Rossi, S. Lee, N. Krajicka, N. D. Spencer, *J. Phys. Chem. C* **2009**, *113*, 16262.
[2] E. Okamoto, K. Yokuyama, K. Tanigawa-Kodaira, N. Ikeda, Y. Kitamoto, T. Ohta, T. Horiba, M. Okamoto, *Phys. Chem. Chem. Phys.* **2010**, *12*, 5218.
[3] N. Ikeda, A. Terfort, M. Zharnikov, *Langmuir* **2004**, *20*, 9180.
[4] M. Zharnikov, S. Frey, H. Rong, Y. J. Yang, K. Heister, M. Grunze, E. V. Kolondra, D. L. Frenchetter, Y. M. Lee, E. L. Wysocki, N. R. Armstrong, *J. Phys. Chem. C* **2008**, *112*, 20033.
[5] S. Frey, K. Heister, M. Zharnikov, M. Grunze, K. Tamada, T. Colorado, R. Colorado, H. R. Graupe, J. R. Lee, F. A. Lee, N. R. Armstrong, *J. Phys. Chem. B* **2003**, *107*, 11696.
[6] M. Kind, C. Woll, *Progress in Surface Science* **2009**, *84*, 230.
[7] C. C. Perry, S. Haq, *Surface Science* **2003**, *532–535*, 466.
[8] A. Shaporenko, J. Cyganik, S. Uppili, A. Terfort, M. Zharnikov, *J. Phys. Chem. B* **2005**, *109*, 25633.
[9] A. Shaporenko, A. Ulman, A. Terfort, M. Zharnikov, *J. Electron Spectrosc. Relat. Phenom.* **2005**, *150*, 1.
[10] A. Shaporenko, A. Terfort, M. Zharnikov, *J. Phys. Chem. A* **2007**, *111*, 10179.
[11] A. Ulman, *Chem. Rev.* **1996**, *96*, 1533.
[12] J. C. Love, L. A. Estroff, J. K. Kriebel, R. G. Nuzzo, G. M. Whitesides, *Chem. Rev.* **2005**, *105*, 1103.
[13] F. Schreiber, *Progress in Surface Science* **2000**, *65*, 151.
[14] H. Ron, I. Rubinstein, *Langmuir* **1994**, *10*, 4566.
[15] M. Zharnikov, A. Shaporenko, L. Buck, E. Kessler, *Langmuir* **2004**, *20*, 3748.
[16] M. Zharnikov, S. Frey, K. Heister, M. Grunze, *Langmuir* **2000**, *16*, 2697.
[17] M. Zharnikov, M. Grunze, *J. Vac. Sci. Technol. B* **2001**, *19*, 1797.

§Sandia National Laboratories is a multi-program laboratory operated by Sandia Corporation, a wholly owned subsidiary of Lockheed Martin Corporation, for the U.S. Department of Energy's National Nuclear Security Administration under contract DE-AC04-94AL85000.

Sandia National Laboratories